

Theoretical study of femtosecond photoionization for the Na₂ molecule

Di Yang^{a,b}, Shu-Lin Cong^a, and Ke-Li Han^{b,*}

^a*School of Physics and Optoelectronic Technology, Dalian University of Technology, Dalian 116024, China*

^b*State Key Laboratory of Molecular Reaction Dynamics, Dalian Institute of Chemical Physics, Chinese Academy of Sciences, Dalian 116023, China*

Received 6 May 2010; Accepted (in revised version) 2 June 2010

Published Online 28 June 2010

Abstract. Multiphoton ionization of the Na₂ molecule by a single phase shaped femtosecond laser pulse has been theoretically studied using time-dependent quantum wave packet method including the effect of molecular rotation. We analyze the temporal development of the population and further discuss the molecular motion by mapping the rovibrational wave packet propagation in the excited state. The calculated results show a strong dependence of the kinetic energy-resolved photoelectron spectra on the laser chirp directions and the pulse duration.

PACS: 33.80.Rv

Key words: multiphoton ionization, photoelectron spectra, time-dependent wave packet, effect of rotation

1 Introduction

With the rapid development of laser technology, femtosecond laser pulses have opened the possibility to observe or to control the real-time molecular dynamics [1,2]. Compared to atoms, molecules exhibit complex behavior due to their multi-center nature, which introduces additional vibrational and rotational degrees of freedom. Many interesting phenomena, such as bond softening and hardening [3,4], above-threshold ionization (ATI) and dissociation (ATD) [5,6], adiabatic passage of light-induced potentials (APLIP) [7], and more, have been explored. To illustrate the matter-field interaction process, femtosecond pump-prob photoelectron spectroscopy has become a useful tool in ultrafast molecule science [8,9]. As a prototype, a large number of experimental and theoretical

*Corresponding author. *Email address:* k1han@dicp.ac.cn (K. L. Han)

studies using the pump-prob technology have been made on dynamics of the sodium dimer in laser fields [10–13].

In Ref. [14], the authors reported the observation of the coherent control of the Na₂ molecular multi-photon ionization process in a single phase shaped pulse experiment, where the carrier frequency ω_0 is 618 nm. In the experiment, starting from a Fourier-transform limited 40 fs pulse, either an up-chirp (+3500 fs²) or a down-chirp (-3500 fs²) is introduced. The measured kinetic energy photoelectron spectra showed a strongly chirp- and pulse-duration-dependent behavior and revealed that for down-chirp the population in neutral state may be higher, but the up-chirp led to a higher ionization yield.

In present work, we theoretically stimulate the Na₂ molecular multi-photon ionization process in Ref. [14] including the effect of rotation using time-dependent quantum wave packet method. As the torque exerted by laser fields on molecules can lead to molecular alignment, the effect of rotation should be taken into account to obtain quantitative agreement with experiment. In Ref.[14], the photoelectron spectra had been calculated using time-dependent perturbation theory [13,15]. Compared with their work, the dynamics of the Na₂ molecule is dealt with accurate non-perturbation quantum mechanics method in this letter. The paper is organized as follows: in Section 2, the theoretical method is summarized. The numerical results and their discussions are presented in Section 3, and Section 4 contains the conclusion.

2 Theoretical method

In accordance with the experimental conditions the calculations are performed include four electronic states, the ground state X ¹Σ_g⁺, A ¹Σ_u⁺, 2 ¹Π_g, and the ionic ground state Na₂⁺ ²Σ_g⁺, as shown in Fig. 1. For convenience we refer to the four electronic states as |X⟩, |A⟩, |2⟩, and |I⟩ states, respectively. The nuclear wave functions Ψ are obtained by solving the time-dependent Schrödinger equation

$$i\hbar \frac{\partial}{\partial t} \Psi(R, \theta, t) = [\hat{T}(R, \theta) + \hat{V}(R, \theta, t)] \Psi(R, \theta, t), \quad (1)$$

with

$$\Psi = \begin{pmatrix} \Psi_X \\ \Psi_A \\ \Psi_2 \\ \Psi_I \end{pmatrix}. \quad (2)$$

In this work we consider the initial magnetic quantum number M of the Na₂ molecule to be zero. In the linearly polarized laser field, M is conserved, which is equivalent to ignoring the ∂_ϕ term (ϕ azimuthal angle) in a full three-dimension Hamiltonian. Then the kinetic energy operator $\hat{T}(R, \theta)$ can be expressed as [16,17]

$$\hat{T}(R, \theta) = -\frac{\hbar^2}{2m} \frac{\partial^2}{\partial R^2} - \frac{\hbar^2}{2mR^2} \frac{1}{\sin\theta} \frac{\partial}{\partial \theta} (\sin\theta \frac{\partial}{\partial \theta}), \quad (3)$$

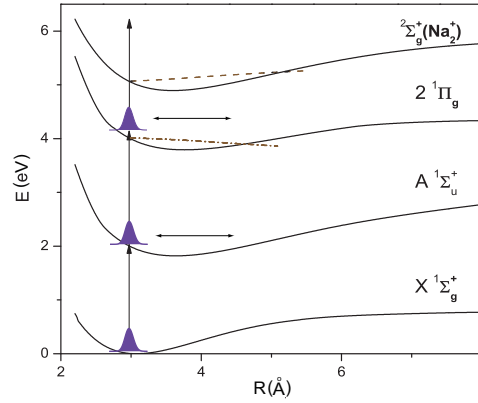


Figure 1: Illustration of the ionization process and the potential energy surfaces of the Na₂ molecule. The dashed line shows the difference potential $|I\rangle - |2\rangle + 2\hbar\omega$. The dash-dotted line shows the difference potential $|2\rangle - |A\rangle + \hbar\omega$.

where m is the reduced mass, R is the internuclear distance, and θ is angle between the laser field direction and the molecular axis. The potential matrix $\hat{V}(R, \theta, t)$ can be written as

$$\hat{V}(R, \theta, t) = \begin{pmatrix} V_X & W_{XA} & 0 & 0 & \cdot & \dots & 0 \\ W_{AX} & V_A & W_{A2} & 0 & \cdot & \dots & 0 \\ 0 & W_{2A} & V_2 & W_{2I} & \cdot & \dots & W_{2I} \\ 0 & 0 & W_{I2} & V_I + E_1 & 0 & \dots & \cdot \\ \cdot & \cdot & \cdot & 0 & V_I + E_2 & 0 & 0 \\ \vdots & \vdots & \vdots & \vdots & 0 & \ddots & 0 \\ 0 & 0 & W_{I2} & 0 & 0 & 0 & V_I + E_N \end{pmatrix}, \quad (4)$$

where V_X, V_A, V_2 and V_I represent the potential energies of different electronic states in the absence of laser field. For $|I\rangle$ state, there are N discrete free-electron-ion pair states detached. Here N is optimally taken as 100. $E_N (N = 1, 2, \dots, 100)$ are the electron kinetic energies of the ionic ground state, and $V_I + E_N (N = 1, 2, \dots, 100)$ denote the total energies of the discrete set of continuum states in the part of ion-pair states.

In Eq. (4), the off-diagonal elements represent the laser-molecule interaction, they are given by

$$W_{XA} = W_{AX} = -\mu_{XA} E(t) \cos\theta, \quad (5)$$

$$W_{A2} = W_{2A} = -\mu_{A2} E(t) \sin\theta, \quad (6)$$

$$W_{2I} = W_{I2} = -\mu_{2I} E(t) \sin\theta. \quad (7)$$

Note the difference in angular dependence between W_{XA} and $W_{A2} (W_{2I})$ because $|A\rangle \leftarrow |X\rangle$ is a parallel transition and $|2\rangle \leftarrow |A\rangle (|I\rangle \leftarrow |2\rangle)$ is a perpendicular transition [18]. The shape of a unchirped laser pulse is chosen as $E(t) = \varepsilon f(t) \cos(\omega t)$, where $f(t) =$

$\exp(-4\ln 2(t/T)^2)$ is the pulse envelope function, ε the peak intensity, ω the central frequency, and T is the full width at half maximum (FWHM) of the pulse. The electric fields of the up-chirped and down-chirped laser pulses are taken from Ref. [19] in the analytical expressions. All of the laser parameters are the same as those of the experiment. We employ the R -dependent transition dipole moments μ_{XA} and μ_{A2} given by Konowalow *et al.* [20]. The coupling strengths between the bound states and the continuum states are much smaller than those between the bound states, and they are always considered to be about a factor of 10 lower than the coupling strengths between the ground and excited states [21].

Before propagating the wave function, its initial form is chosen to be the rovibrational eigenfunction of the ground state $|X\rangle$. Here we use the discrete variable representation (DVR) method to obtain the radial vibrational eigenfunction [22]. The Legendre polynomials $P_J(\cos\theta)$ are employed as eigenfunctions for the angular part. Then the initial rovibrational eigenfunction is a direct product of the radial part and the angular part [17,23]. The time propagation is accomplished using the split-operator method [24]. The time-dependent population in the electronic $|2\rangle$ state is obtained from the calculation

$$\mathcal{P}_2(t) = \int d\theta \sin\theta \int dR |\Psi_2(R, \theta, t)|^2, \quad (8)$$

and the energy-resolved photoelectron spectrum is defined as

$$\mathcal{P}_I(E_N) = \lim_{t \rightarrow \infty} \int d\theta \sin\theta \int dR |\Psi_I(R, \theta, E_N, t)|^2. \quad (9)$$

3 Results and discussion

The ionization scheme and the relevant potential energy curves of the Na_2 molecule are depicted in Fig. 1. At the center wavelength of the laser pulse 618nm the Na_2 molecule is ionized from its neutral ground state $|X\rangle$ into its ionic ground state $|I\rangle$ via two resonant states. Under the Franck-Condon principle, one-photon excitation leads to a wave packet at the inner turning point of the $|A\rangle$ state potential. Then a wave packet is prepared at the inner turning point of the $|2\rangle$ state potential by two-photon absorption. The dash-dotted line in Fig. 1 displays the difference potential $|2\rangle - |A\rangle + \hbar\omega$ and the dashed line indicates the difference potential $|I\rangle - |2\rangle + 2\hbar\omega$ relevant for the 'direct' photoionization process. It is well known that the electrons of different kinetic energies are released at different internuclear coordinates.

The simulated photoelectron spectra and that obtained from experiment as well as the results of their theoretical study [14] are displayed in Fig. 2. To sum up the comparison between our predicted results including the effect of rotation and the presented in Ref. [14], the agreement of our calculated results with the experimental one is fairly satisfactory, both in ionization yield and in the kinetic energy distribution of the photoelectrons. Two characters of the spectra can be derived explicitly from Fig. 2(c). Firstly, the ionization yield is higher for up-chirped than for down-chirped laser pulses. Secondly, the

electron energy distribution with unchirped laser pulse is shifted towards higher energies than the chirped pulse ($\pm 3500 \text{ fs}^2$) electron spectra.

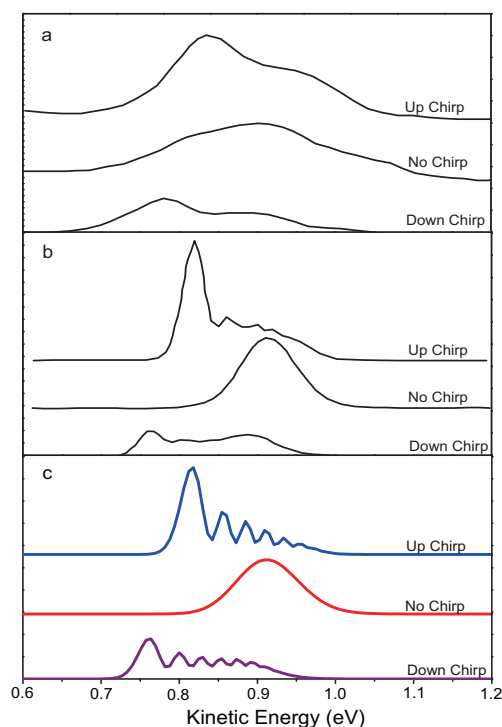


Figure 2: (a) Electron spectra measured in Ref. [14] with single up-chirped ($+3500 \text{ fs}^2$), down-chirped (-3500 fs^2) and unchirped laser pulses. The transform-limited pulses of 40 fs duration are centered at a wavelength of 618 nm. The chirped pulses are of 240 fs duration. (b) Calculated spectra in Ref.[14] with perturbation theory. (c) Simulated spectra with the quantum wave packet method in this work using the same parameters as above.

In order to explain the first character we obtain the time-dependent population of the $|2\rangle$ state, which is directly coupled to the discretized continuum of the ionic ground state $|I\rangle$, for both up- and down-chirped laser pulses. The result is exhibited in Fig. 3(a). It is clearly seen that the up-chirped laser pulse (red frequencies first) transfers population from the $|A\rangle$ state to the $|2\rangle$ state earlier than the down-chirped laser pulse (blue frequencies first). Because the Frank-Condon overlap maximum for the $|2\rangle \leftarrow |A\rangle$ state transition is shifted towards the red of the central laser wavelength. Since the ionization from the temporal wings of the pulse is small with the main contribution coming from the peak of the pulse [25], the high ionization yield is achieved with up-chirped pulse, which transfers high population in the $|2\rangle$ state at the maximum laser intensity ($t=0 \text{ fs}$), but not with down-chirped laser pulse. It is another interesting phenomenon in Fig. 3(a) that the total population in the $|2\rangle$ state after the end of pulse is larger for the down-chirped laser. This finding can be interpreted by the semiclassical difference potential analysis. Taking Mulliken's difference potential principle into account [26], as for the down-chirped pulse, the decreasing photon energy in time follows the decrease in the difference potential be-

tween the $|2\rangle$ state and the $|A\rangle$ state as the wave packet of the $|A\rangle$ state moves to larger internuclear distances (see Fig. 1), the excitation is more efficient. The calculated result from Ref. [14] is available in the inset. Our calculations are closely in agreement with them. As Assion *et al.* pointed out that the kind of optimization is desired in coherent control schemes [14]. That is to say the up-chirped laser pulse minimize the population remaining in the excited state and maximize simultaneously the yield of the final product Na_2^+ . The results are displayed in Fig. 3(b).

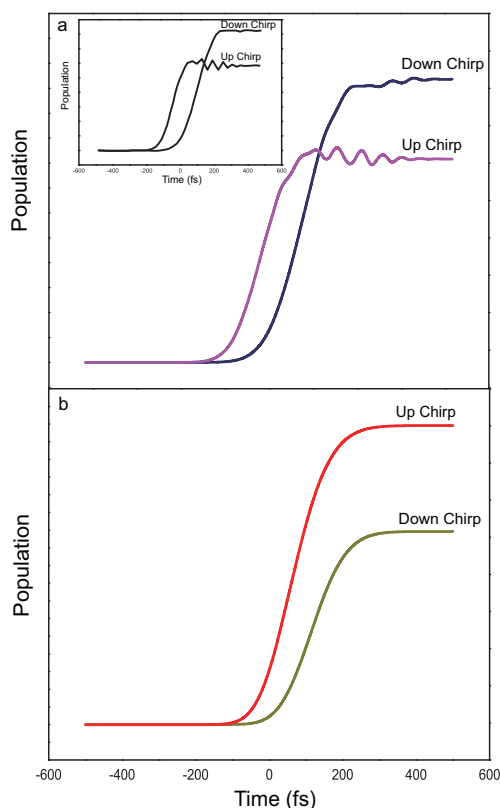


Figure 3: Calculated the time-dependent populations in (a) the $|2\rangle$ state and (b) the $\text{Na}_2^+ |I\rangle$ state with up- and down-chirped laser pulses. The result of Ref.[14] is in the inset. The laser parameters are the same as those in Fig. 2.

With regard to the second character, combining the difference potential analysis and the time-resolved wave packet theory, we can understand the different electron signal for upchirped 40 fs laser pulse compared to the chirped laser pulses of 240 fs duration. One peak around 0.9 eV is observed in the spectra for the short laser pulse, however the longer pulses yield electrons with kinetic energy of about 0.8 eV or less (see Fig. 2(c)). A more detailed picture about the wave packet dynamics in the $|2\rangle$ state is presented in Fig. 4. We can draw the main conclusion easily from it. The identical duration of about 240 fs for the up- and down-chirped laser pulses allows the wave packet to sweep the wide

range of the internuclear distances. But the unchirped laser pulse is of much shorter duration. Therefore the wave packet has no time to move to large internuclear distances during the ionization process. On the other hand the difference potential between the ionic ground state $|I\rangle$ and the excited $|2\rangle$ state is increasing with increasing internuclear distance, which results in the corresponding electron energy decreasing. In other words, the electron formed at the outer turning point has less kinetic energy than that formed at the inner turning point (see Fig. 1). So, the fast electrons are from the unchirped pulse and the photoelectrons with broad energy distribution are released from the chirped pulses.

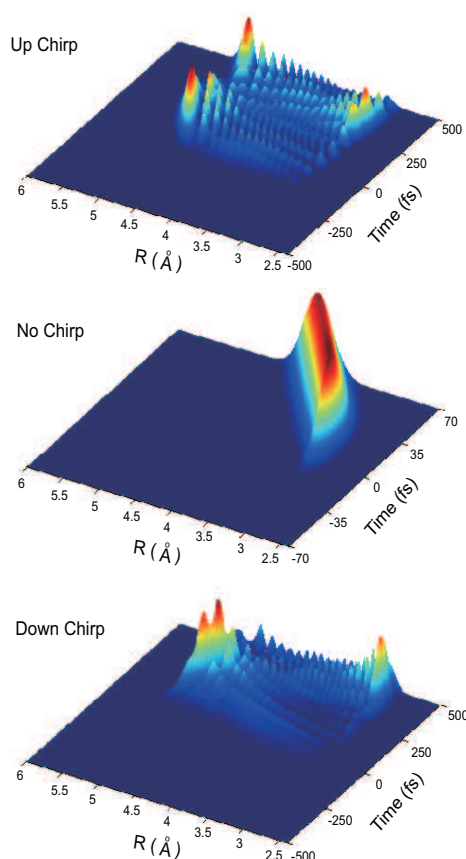


Figure 4: The evolutions of the wave packets in the $|2\rangle$ state during interaction with up-chirped, unchirped and down-chirped laser pulses. The laser parameters are the same as those in Fig. 2.

In the above calculations, the initial wave function is chosen to be the rovibrational eigenfunction $|v,j\rangle = |0,0\rangle$ of the ground $|X\rangle$ state. It is well known that the initial rotational populations in the ground vibrational state of the ground $|X\rangle$ state at one rotational temperature comply with the Boltzmann distribution. Furthermore we simulate the photoelectron spectra at an initial rotational temperature $T = 10$ K by adding up the results from different rovibrational states of the $|X\rangle$ state scaled by the Boltzmann distribution

, respectively. The calculations, which are not presented here, show that the different initial rotational states can only change the intensity of spectra without affecting the patterns of the photoelectron signals. Here we demonstrate the time-dependent angular distributions in the $|2\rangle$ state with initial $J_0 = 0, 3, 6$ for both laser chirps in Fig. 5. As shown in this figure, the higher initial rotational quantum numbers, the more population will be transferred to the $|2\rangle$ state around $\theta \approx 0$ and π . At the same time the temporal angular distributions obviously verify that the up-chirped laser pulse transfers population $|2\rangle \leftarrow |A\rangle$ earlier than the down-chirped laser pulse.

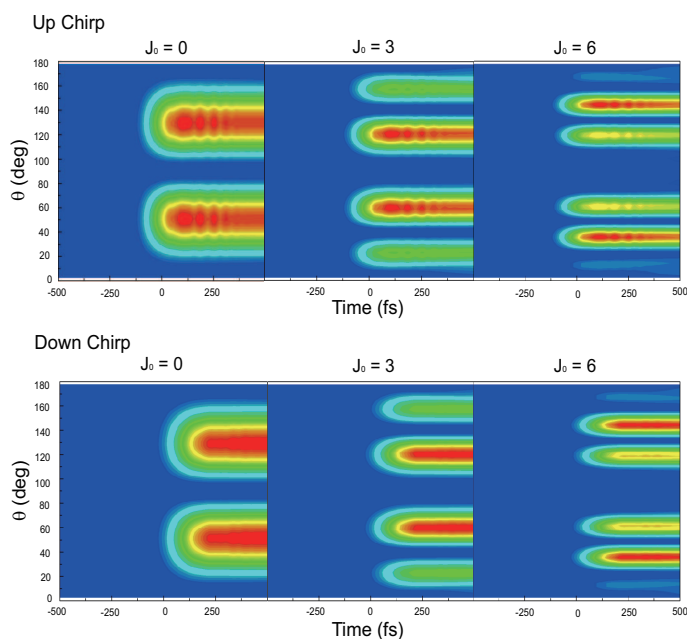


Figure 5: Contour plot of the temporal angular distribution in the $|2\rangle$ state with initial rotational state $J_0 = 0, 3, 6$ during interaction with up-chirped and down-chirped laser pulses. The laser parameters are the same as those in Fig. 2.

4 Conclusion

We have theoretically investigated the coherent control of the Na_2 molecule multiphoton ionization process using chirped femtosecond laser pulses. The time-dependent wave packet method with the effect of molecular rotation is used to numerically simulate the photoelectron kinetic energy spectra. It is found that both the pulse duration and the phase modulation of the ultrashort laser pulse can strongly affect the resonance enhanced multiphoton ionization process and our results agree well with the experimental measurements. In addition, we choose different rotational quantum numbers in the initial rovibrational wave function to test the reliability of our results. It is noted that the effect of the initial thermal rotational distribution does not change the main results.

References

- [1] B. M. Garraway and K. -A. Suominen, Rep. Prog. Phys. 58 (1995) 365.
- [2] B. M. Garraway and K. -A. Suominen, Contemp. Phys. 43 (2002) 97.
- [3] P. H. Bucksbaum, A. Zavriyev, H. G. Muller, *et al.*, Phys. Rev. Lett. 64 (1990) 1883.
- [4] L. J. Frasinski, J. H. Posthumus, J. Plumridge, *et al.*, Phys. Rev. Lett. 83 (1999) 3625.
- [5] R. R. Freeman, P. H. Bucksbaum, H. Milchberg, *et al.*, Phys. Rev. Lett. 59 (1987) 1092.
- [6] A. Zavriyev, P. H. Bucksbaum, H. G. Muller, *et al.*, Phys. Rev. A 42 (1990) 5500.
- [7] B. M. Garraway and K. -A. Suominen, Phys. Rev. Lett. 80 (1998) 932.
- [8] M. Wollenhaupt, V. Engel, and T. Baumert, Annu. Rev. Phys. Chem. 56 (2005) 25.
- [9] T. Frohnmeyer and T. Baumert, Appl. Phys. B 71 (2000) 259.
- [10] T. Baumert, B. Bühler, R. Thalweiser, *et al.*, Phys. Rev. Lett. 64 (1990) 733.
- [11] T. Baumert, M. Grosser, R. Thalweiser, *et al.*, Phys. Rev. Lett. 67 (1991) 3753.
- [12] C. Meier and V. Engel, Chem. Phys. Lett. 212 (1993) 691.
- [13] V. Engel, T. Baumert, C. Meier, *et al.*, Z. Phys. D, 28 (1993) 37.
- [14] A. Assion, T. Baumert, J. Helbing, *et al.*, Chem. Phys. Lett. 259 (1996) 488.
- [15] C. Meier and V. Engel, Pump-probe ionization spectroscopy of a diatomic molecule: the sodium dimer as a prototype example, in: Femtosecond Chemistry, eds. J. Manz and L. Woeste (VCH, Weinheim, 1995) pp. 369.
- [16] R. Numico, A. Keller, and O. Atabek, Phys. Rev. A 52 (1995) 1298.
- [17] M. Y. Zhao, Q. T. Meng, T. X. Xie, *et al.*, Int. J. Quantum Chem. 101 (2005) 153.
- [18] S. Gröfe, M. Erdmann, and V. Engel, Phys. Rev. A 72 (2005) 013404.
- [19] M. Krug, T. Bayer, M. Wollenhaupt, *et al.*, New J. Phys. 11 (2009) 105051.
- [20] D. D. Konowalow, M. E. Rosenkrantz, and D. S. Hochhauser, J. Mol. Spectrosc. 99 (1983) 321.
- [21] T. Baumert, V. Engel, C. Meier, *et al.*, Chem. Phys. Lett. 200 (1992) 488.
- [22] J. Hu, K. L. Han, and G. Z. He, Phys. Rev. Lett. 95 (2005) 123001.
- [23] K. J. Yuan, Z. G. Sun, S. L. Cong, *et al.*, Phys. Rev. A 74 (2006) 043421.
- [24] J. Hu, Q. T. Meng, and K. L. Han, Chem. Phys. Lett. 393 (2004) 393.
- [25] G. N. Gibson, R. R. Freeman, and T. J. McIlrath, Phys. Rev. Lett. 69 (1992) 1904.
- [26] R. S. Mulliken, J. Chem. Phys. 55 (1997) 309.